

# Evaluation of the efficiency potential of intermediate band solar cells based on thin-film chalcopyrite materials

Antonio Martí, David Fuertes Marrón,<sup>a)</sup> and Antonio Luque

*Instituto de Energía Solar-ETSIT, Universidad Politécnica de Madrid, Ciudad Universitaria sn, 28040 Madrid, Spain*

(Received 5 October 2007; accepted 21 January 2008; published online 2 April 2008)

This paper discusses the potential of the intermediate band solar cell (IBSC) concept to improve the efficiency of thin-film chalcopyrite solar cells. The results show that solar cells based on CuGaS<sub>2</sub>, with a radiative limiting efficiency of 46.7%, exhibit the highest potential. A simple method for the identification of transition elements that when incorporated in CuGaS<sub>2</sub> could possibly introduce an intermediate band is also described. The IBSC concept is also applied under the assumptions that thin-film solar cells are not to be operated under concentrated light and that a non-negligible contribution of nonradiative recombination exists. © 2008 American Institute of Physics. [DOI: 10.1063/1.2901213]

## I. INTRODUCTION

The intermediate band solar cell (IBSC) concept was proposed<sup>1</sup> as a concept to increase the efficiency of single gap solar cells. In this paper, we specifically discuss the potential of this concept to increase the efficiency of thin-film solar cells and, in particular, of some based on I-III-VI<sub>2</sub> compounds. Two aspects are specific for the application of the IBSC concept to thin films. First, thin-film materials are, in principle, not intended to be used under highly concentrated light<sup>2</sup> and, therefore, the study of their potential should be carried out at the level of irradiance of 1 sun. Section III of this paper is devoted to the discussion of this particular aspect. Also, in this respect, the potential of transition elements to create an intermediate band (IB) is sought in Sec. III. Second, despite a remarkable electronic tolerance to hosting point defects<sup>3</sup> and the relative benign character of grain boundaries of polycrystalline samples,<sup>4</sup> actual thin-film chalcopyrite materials are characterized by a high density of defects introducing nonradiative recombination. This implies that their operation is far from the radiative limit assumed when calculating the limiting efficiency of the IBSC. The consequences of this fact are discussed in Sec. IV by studying the potential for improvement of a Cu(In,Ga)Se<sub>2</sub> solar cell.

## II. LIMITING EFFICIENCY OF THE IBSC CONCEPT FOR OPERATION AT 1 SUN

Conceptually, an IBSC is manufactured by sandwiching an IB material in-between two emitters, one of *p* type and the other of *n* type (Fig. 1). The IB material is characterized by the existence of an electronic energy band of allowed states within the conventional bandgap  $E_G$ , splitting it into two subgaps,  $E_L$  and  $E_H$ . This band allows the creation of additional electron-hole pairs from the absorption of two sub-bandgap energy photons. Under this assumption, one photon pumps an electron from the valence band (VB) to the IB

(photon 1) and a second photon (photon 2) pumps an electron from the IB to the conduction band (CB). To this end, it is necessary that the IB is half-filled with electrons so that it can supply electrons to the CB as well as receive them from the VB. This two-photon absorption process is also illustrated in Fig. 1 and has been experimentally detected in IBSCs based on quantum dots.<sup>5</sup> The electron-hole pairs generated in this way add up to the conventionally generated ones by the absorption of a single photon pumping an electron from the VB to the CB (photon 3). Therefore, the photocur-

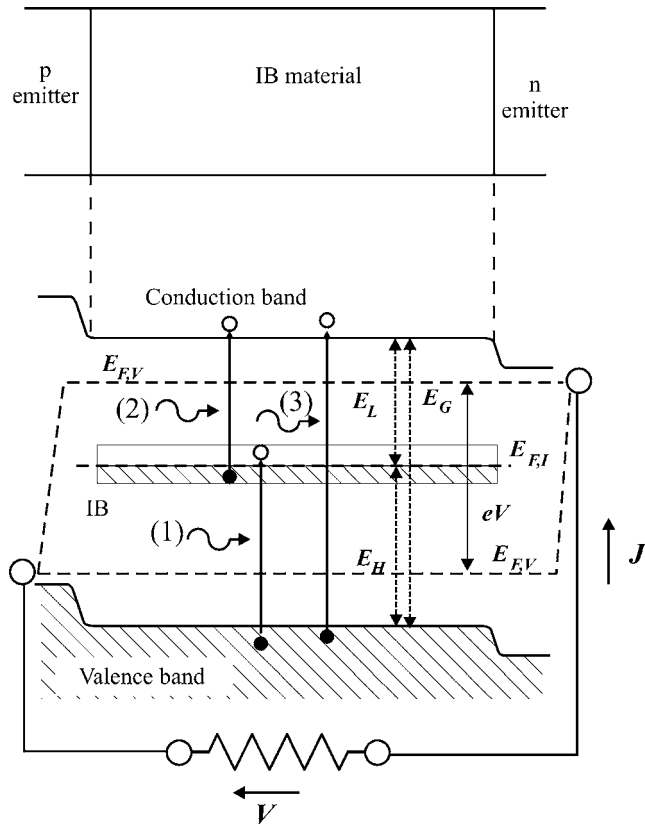


FIG. 1. General structure of an IBSC showing the energy gaps and photon absorption processes involved.

<sup>a)</sup>Electronic mail: dfuertes@ies-def.upm.es.

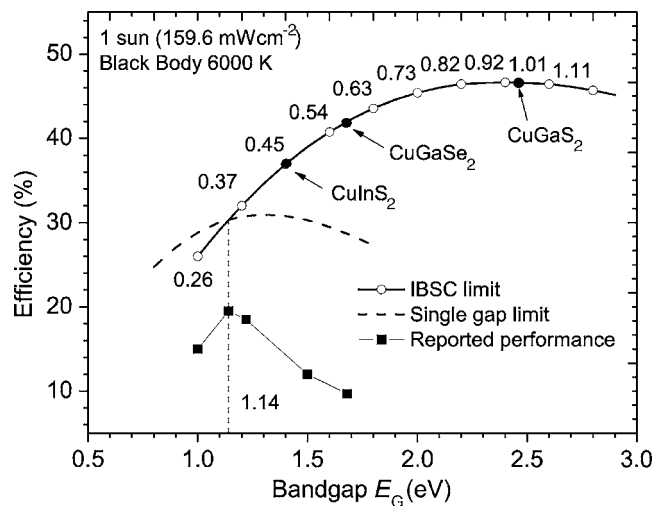


FIG. 2. Limiting efficiency of an IBSC when operated at 1 sun as a function of the total semiconductor bandgap  $E_G$ . Figures in the plot indicate the optimum value (in eV) of the subbandgap  $E_L$ . The limiting efficiency of single gap solar cells is also shown for comparison (dashed line), as well as the reported state of the art (under AM1.5G) of Cu-containing, chalcopyrite-based solar cells (solid squares, adapted from Ref. 15).

rent of the solar cell, and ultimately its efficiency, are enhanced since this increment in photocurrent occurs without degradation of the output voltage of the cell. This output voltage is given by the split between electron and hole quasi-Fermi levels,  $E_{FC}$  and  $E_{FV}$ , that is still limited by the total bandgap  $E_G$ . A more complete description of this theory has already been described elsewhere<sup>1,6–8</sup> and will not be repeated here. Nevertheless, it is worth mentioning that the presence of the intermediate band relaxes the main constraint imposed on the conventional two-photon absorption process, as first described by Göppert-Mayer,<sup>9</sup> which requires the *simultaneous* absorption of the two photons allowing the electronic transition via a virtual state. Indeed, this effect contributes to nonlinear optical limiting observed in optoelectronic materials under high intensity irradiation<sup>10</sup> and is commonly used in fluorescence microscopy.<sup>11</sup>

Calculations for the limiting efficiency of the IBSC concept are usually carried out at maximum light concentration. Since it is our purpose to study the potential of thin-film, IBSCs, it is convenient to review the limiting efficiency of this concept when the cells are operated at 1 sun. The results in this respect are plotted in Fig. 2. They have been obtained assuming the sun as a black body (BB) at 6000 K. At this stage, this choice of the spectrum makes the comparison between different results easier when it comes to the calculation of limiting efficiencies (discussions concerning the use of AM1.5 Global spectrum will come later). Concerning the recombination of minority carriers, this is assumed to be completely radiative with the recombination rate related to the photon absorption coefficient through the van Roosbroeck–Shockley model.<sup>12</sup>

Limiting efficiencies in Fig. 2 have been plotted as a function of the total bandgap  $E_G$ . The corresponding optimum value for  $E_L$ , in eV, is also given. It must be remembered that, for example, a value  $E_L=0.80$  eV implies that the optimum position of the IB is located either 0.8 eV from the

CB or from the VB. The limiting efficiency for single gap solar cells, which is obtained using detailed balance arguments,<sup>13,14</sup> is also plotted for reference, as well as the reported state of the art of Cu-containing, chalcopyrite-based solar cells (solid squares, under AM1.5G, adapted from Ref. 15).

Two important results can be drawn from the analysis of this plot. First, the optimum gap for photovoltaic energy conversion at 1 sun appears at 2.41 eV with the IB located at 0.92 eV from the CB (or VB) ( $E_L=0.92$  eV) and exhibiting a potential efficiency of 46.77%. In this sense, CuGaS<sub>2</sub>, with a bandgap of 2.46 eV (Ref. 16) and a limiting efficiency of 46.73% approaches this optimum well. This compound has indeed been proposed for optoelectronic devices,<sup>17</sup> although its applicability for solar cells in conventional single gap devices appears limited by the wide bandgap (see Fig. 2). The efficiency potential of other I-III-VI<sub>2</sub> based solar cells, with bandgaps away from the optimum, is also shown for reference (black dots). Alloys of the type Cu(In,Ga)(S,Se)<sub>2</sub> would further allow to track the curve of the potential efficiency at the desired bandgap.

The second result is related to the fact that, for bandgaps  $E_G < 1.14$  eV, no improvement is obtained from the insertion of an IB inside the semiconductor bandgap. The physical reason for this is that, for low values of the bandgap, the single gap solar cell already produces a significant photocurrent by itself. Then, although the insertion of an IB may have the potential to further improve this photocurrent, this improvement is, in turn, compensated by the recombination (even being only radiative) that the IB introduces.

The above calculations are only valid in the radiative limit. Practical thin-film solar cells are still far from operating at this limit and, therefore, here, the results shown should be understood as a guidance to approach the maximum efficiency by knowing which combinations of bandgaps exhibit the highest room for improvement. Within this framework, we will also attempt to identify in the next section what elements could lead to the formation of an IB in these compounds.

### III. TRANSITION METALS AS PRECURSORS OF INTERMEDIATE BAND MATERIALS

The incorporation of appropriate impurities in the semiconductor bulk and with the sufficient density has been proposed as a means to engineer IB materials.<sup>7</sup> By “appropriate impurities” we mean impurities that introduce energy levels within the semiconductor bandgap at the energy position required by the IBSC theory in order to maximize the solar cell efficiency. On the other hand, a “sufficient density” implies a density of states enough to allow for the Mott transition, at which the electron wave function changes from localized to delocalized type. Nonradiative recombination is believed to be inhibited when this transition takes place. Other suggested procedures include the use of quantum dots<sup>18</sup> and the exploitation of the band-anticrossing phenomena.<sup>19,20</sup> Here, we will focus on the first approach in order to predict what elements, when incorporated in a CuGaS<sub>2</sub> matrix, could create an IB at its optimum position. The choice of CuGaS<sub>2</sub> is motivated, as

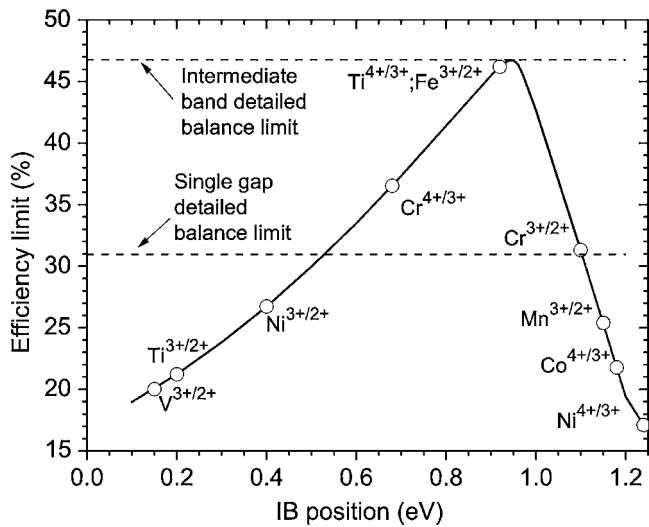


FIG. 3. Limiting efficiency of a CuGaS<sub>2</sub> solar cell as a function of the position of the IB measured from the CB or from the VB indistinguishably. The position of the energy level predicted for some transition elements is also indicated.

explained in the previous section, by the fact that it possesses an optimum bandgap for IBSC operation. In this respect, Fig. 3 plots the limiting efficiency of an ideal IBSC based on CuGaS<sub>2</sub> operating in the radiative limit as a function of the position of the IB.

Concerning the energy levels that transition elements introduce in semiconductors, it has been found that, in III-V and II-VI compounds,<sup>21–23</sup> these energy levels are independent of the semiconductor host when they are referred to some absolute energy value, namely, the vacuum level. In this section, we will use this result as a rough guidance to estimate the energy levels that certain transition elements would introduce in CuGaS<sub>2</sub> by assuming that this rule would also apply to some extent to I-III-VI<sub>2</sub> compounds. No claim is made in this respect about the accuracy of the estimated positions of the corresponding levels, which should certainly be obtained from more elaborated *ab initio* calculations, but rather serve as a first screening in the case that these calculations were to be performed.

We will take, as starting point, the energy position that the transition elements produce in GaAs. This position has been obtained from the review by Hennel<sup>24</sup> and has been summarized in Table I. In this respect, if *X* is the given

TABLE I. Energy levels introduced by different transition elements in GaAs and predicted position in CuGaS<sub>2</sub>. Figures are given relative to the valence band edge.

	GaAs		CuGaS <sub>2</sub>	
	Donor (eV)	Acceptor (eV)	Donor (eV)	Acceptor (eV)
V	...	1.27	...	2.31
Ti	0.50	1.22	1.54	2.26
Cr	0.32	0.74	1.36	1.78
Fe	...	0.5	...	1.54
Co	0.14	1.53	1.18	2.57
Ni	0.20	1.02	1.24	2.06
Mn	...	0.11	...	1.15

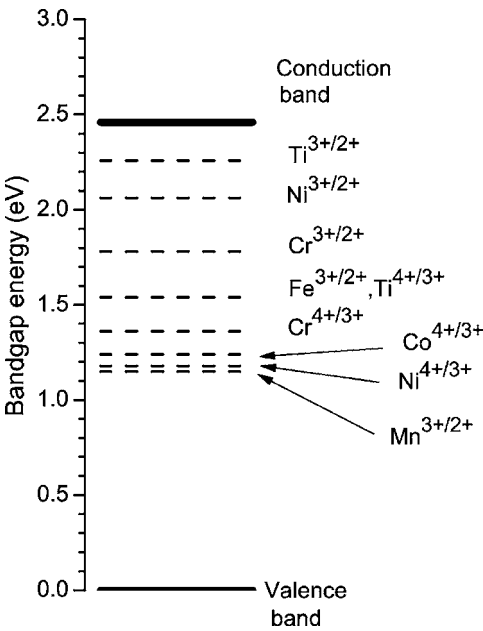


FIG. 4. Predicted energy levels in CuGaS<sub>2</sub> for different transition elements.

transition element, only donor (*X*<sup>4+/3+</sup>) and single acceptor levels (*X*<sup>3+/2+</sup>, following the same nomenclature as used by Hennel) will be considered here. It is further assumed that, when introduced in CuGaS<sub>2</sub>, these levels preserve their character as when substituting Ga positions in GaAs. If *E<sub>H</sub>*(GaAs) is the position of this energy level in GaAs when referred to the valence band, its position in CuGaS<sub>2</sub>, *E<sub>H</sub>*(CuGaS<sub>2</sub>), also referred to the VB, will be given by

$$E_H(\text{CuGaS}_2) = E_H(\text{GaAs}) + \Delta\chi + \Delta E_G, \tag{1}$$

where

$$\Delta E_G = E_G(\text{CuGaS}_2) - E_G(\text{GaAs}) \tag{2}$$

is the difference between gap values and

$$\Delta\chi = \chi(\text{CuGaS}_2) - \chi(\text{GaAs}) \tag{3}$$

is the difference between electron affinities, which we will assume to be approximately zero given the value proposed for CuGaS<sub>2</sub> by Sugiyama and Chichibu<sup>25</sup> (4.1 eV) and the value commonly accepted for GaAs (Ref. 26) (4.07 eV).

Figure 4 illustrates to scale the position of the predicted energy levels within the CuGaS<sub>2</sub> bandgap obtained following this model, assuming complete solubility of the impurities in the chalcopyrite matrix and that they occupy substitutional sites, as described in the paragraph above. As mentioned above, when introduced in sufficiently high density, these levels are expected to lead to the formation of the IB. Figure 3 indicates the limiting efficiency associated with these positions. In this respect, the levels potentially introduced by Ti<sup>4+/3+</sup> and Fe<sup>3+/2+</sup> appear as the most promising ones, leading to optimum locations of the IB. It must be remembered, however, that in order to half-fill this IB with electrons, the introduction of shallow donors (or acceptors) in appropriate amounts may still be required (e.g., at the optimal concentration of that of the transition element concentration multiplied by half the degeneracy of the transition element level, if the considered level were the only one introduced by the

TABLE II. Performance of Cu(InGa)Se<sub>2</sub>.

	$J_{SC}$ (mA cm <sup>-2</sup> )	$V_{OC}$ (V)	$\eta$ (%)
AM1.5G	35.2	0.692	19.8
BB	47.3	0.702	16.9
BB-IBSC	63.9	0.712	23.3
BB-IBSC (overlap)	55.6	0.695	19.2

transition metal). The case of Ti as a potential element leading to the formation of an IB in CuGaS<sub>2</sub> was first identified by Palacios *et al.*<sup>27</sup> using *ab initio* calculations. Other works have addressed the issue of incorporating transition and rare-earth elements in different chalcopyrite compounds for photovoltaic, magnetic, and spintronic applications, both at theoretical<sup>28–30</sup> and experimental levels.<sup>31–36</sup> The reader is referred to these works and to the references therein for details on issues related to the solubility ranges of impurities, defect formation energies, and their impact on the electronic structure of the host compounds, not treated in further detail here.

#### IV. LOW BANDGAP CHALCOPYRITE CELL IN THE PRESENCE OF NONRADIATIVE RECOMBINATION

In the above sections, efficiencies were calculated in the radiative limit, and the potential of the IBSC concept, when the operation of the cell takes place at 1 sun, was determined. From this analysis, it was concluded that little improvement could be expected for cells with low bandgap and, actually, it was found that the introduction of an IB worsens the performance of the cell when the total bandgap of the absorber is lower than 1.14 eV.

However, practical thin-film solar cells do not operate in the radiative limit and the purpose of this section is to determine whether, in this case, it is possible that the creation of an IB can give beneficial results. For carrying out this analysis, we will take as a starting point the reported data from operating Cu(In,Ga)Se<sub>2</sub> solar cells, with a bandgap of 1.14 eV, and characterized by the operation parameters listed in Table II (row labeled “AM1.5G”).

The short-circuit current density chosen for this cell ( $J_{SC}=35.2$  mA cm<sup>-2</sup>) corresponds to the value of the record efficiency solar cell reported by Contreras *et al.*<sup>15</sup> on this material. The illumination spectrum corresponds to AM1.5 Global (1000 W m<sup>-2</sup>) spectrum. The experimental current implies 23.0% of current losses with respect to the maximum achievable<sup>37</sup> (42.7 mA cm<sup>-2</sup>) for a cell of this bandgap and for this spectrum.

The current-voltage  $J(V)$  characteristic of this cell will be modeled by means of the standard equation

$$J = J_{SC} - J_0 \left( \exp \frac{eV}{mkT_C} - 1 \right), \quad (4)$$

neglecting the effect of series and shunt resistance, where  $e$  is the electron charge,  $k$  is Boltzmann’s constant,  $T_C$  is the temperature of operation of the cell (300 K), and  $m$  is the diode ideality factor. We will assume the experimental value<sup>15</sup>  $m=1.3$ , what physically implies that the dominant recombination mechanisms are nonradiative and take place

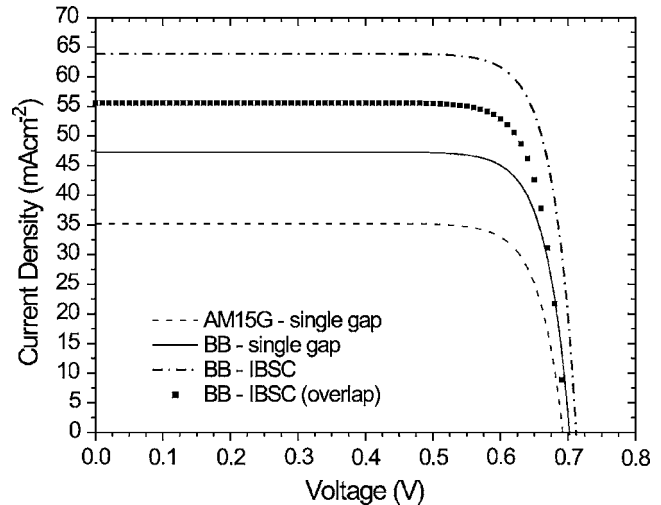


FIG. 5. Current density-voltage characteristic of the same Cu(InGa)Se<sub>2</sub> solar cell, in the presence of nonradiative recombination when illuminated with AM1.5G spectrum (AM1.5G-single gap), BB radiation at 6000 K (BB-single gap), when an IB is inserted (BB-IBSC) at its optimum position ( $E_L=0.37$  eV) and for the case in which the overlap between absorption coefficients exist.

in the space-charge region of the cell. The saturation current density  $J_0$  is set<sup>15</sup> to  $4.0 \times 10^{-8}$  mA cm<sup>-2</sup> which gives the reported open-circuit voltage  $V_{OC}=0.692$  V and an efficiency of 19.8% [for this purpose, we have evaluated numerically the  $J(V)$  curve as to maximize the resulting efficiency, starting from the given values for  $m$ ,  $J_0$ , and  $J_{SC}$ , after obtaining  $V_{OC}$  from the same set of parameters]. This efficiency is slightly higher than the reported recorded efficiency (19.5%) and is due to the fact that we are in this study neglecting series and shunt resistance effects. By this choice, we have selected the “best” reported Cu(In,Ga)Se<sub>2</sub> solar cell<sup>15</sup> for our discussion although, as mentioned, its performance is limited by nonradiative recombination mechanisms. The current density-voltage characteristic, henceforth, obtained from the model set by Eq. (4) is plotted in Fig. 5 (curve labeled “AM1.5G-single gap”). In the next paragraphs, our purpose is to investigate whether the performance of this cell can be improved by the insertion of an IB.

In order to make a fair comparison possible between the efficiency of the cells illuminated under AM1.5G spectrum and the limiting efficiencies calculated in Sec. II, where the cells were studied under black-body (BB) illumination at 6000 K (1595.9 W m<sup>-2</sup>), it is first necessary to calculate the equivalent short-circuit current density of the cell under BB illumination. In this respect, it is found that the short-circuit current density  $J_{SC}=35.2$  mA cm<sup>-2</sup> under AM1.5G illumination is equivalent to 47.3 mA cm<sup>-2</sup> under 1 sun of BB radiation. This figure is the result of calculating the maximum short-circuit current for a solar cell made of a semiconductor with a bandgap of 1.14 eV (61.4 mA cm<sup>-2</sup>) but still assuming 23.0% of losses factor. To calculate the equivalent efficiency, the current-voltage characteristic is then still assumed to be given by Eq. (4) but with the new value for the short-circuit current. The resulting characteristic is plotted in Fig. 5 (BB—single gap) and its corresponding performance parameters have been summarized in Table II (row “BB”). As it



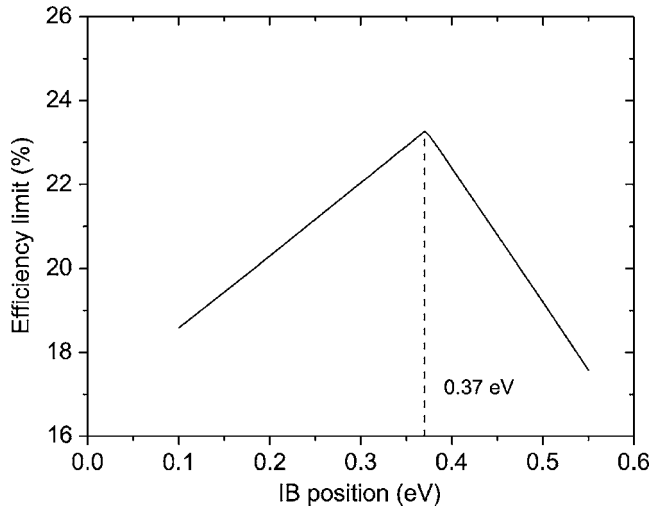


FIG. 6. Efficiency of a Cu(In,Ga)Se<sub>2</sub>-based cell ( $E_G=1.14$  eV), in the presence of nonradiative recombination, as a function of the position of an ideal intermediate band.

can be observed, the mere change of spectrum lowers the efficiency from 19.8% (AM1.5G) to 16.9% (BB) because of a larger blue fraction.

We now will assume that an IB would be inserted in the Cu(In,Ga)Se<sub>2</sub> cell. This IB will be assumed ideal, which, in particular, implies that carriers can go to and exit from the IB only through a radiative generation-recombination process with the CB or the VB. It also implies that electrons in the IB do not undergo transitions to other energy levels that might exist in the cell (and which actually are responsible for the diode factor  $m=1.3$ ). In this sense, carrier generation-recombination from the IB to these centers is disregarded. These interactions could be included in the model by increasing the saturation current  $J_0$  and, possibly, by modifying the ideality factor  $m$ , and would tend to reduce the open-circuit voltage of the cell with respect to the results to be presented here. However, these phenomena would be extremely difficult to model at this stage and, besides, they have been found irrelevant given the final results that will follow when taking into account other considerations. Nevertheless, these idealizations will allow us again to explore the maximum potential of the IBSC approach for the present case.

As far as the extra photogenerated current induced by the IB is concerned, we will still assume that this current cannot be extracted better than with a 23.0% of losses, as for state-of-the-art devices. To account for these losses, we will introduce the dimensionless factor  $\xi=1-0.230=0.770$ . Further details of the model used to obtain the current-voltage characteristic of the cell with IB will be given in the next paragraph. For the moment, Fig. 6 plots the efficiency of the cell as a function of the position of the IB. It is found that the optimum location occurs at 0.37 eV from the CB (or from the VB). The current-voltage characteristic of this cell, with the IB at this position, is plotted in Fig. 5 (curve “BB-IBSC”) and leads to an efficiency of 23.3%. Hence, it can be concluded, that the room for improvement of a practical Cu(In,Ga)Se<sub>2</sub> cell, considering an ideal IB, is 6.4 points (from 16.9% to 23.3%). The rest of the performance parameters are collected in Table II.

In order to detail the mathematical model used to calculate the BB-IBSC characteristic, we will define

$$\dot{N}(E_1, E_2, T, \mu) = \frac{2H}{h^3 c^2} \int_{E_1}^{E_2} \frac{\varepsilon^2}{\exp\left(\frac{\varepsilon - \mu}{kT}\right) - 1} d\varepsilon, \quad (5)$$

$$E_{FC} - E_{FI} = \mu_{CI}, \quad (6)$$

$$E_{FI} - E_{FV} = \mu_{IV}, \quad (7)$$

$$E_{FC} - E_{FV} = \mu_{CV}, \quad (8)$$

where  $H=\pi/46\,050$  the étendue<sup>38</sup> of the sun seen from the cell when no concentration is used,  $h$  is Planck’s constant,  $c$  is the speed of light in vacuum, and  $k$  is Boltzmann’s constant. The current-voltage characteristic  $J(V)$  is then given by

$$J \approx e\xi[\dot{N}(E_L, E_H, T_S, 0) + \dot{N}(E_G, \infty, T_S, 0)] - \left[ e\dot{N}(E_L, E_H, T_C, \mu_{CI}) + e\dot{N}(E_G, \infty, T_C, \mu_{CV}) + J_0 \left( \exp \frac{\mu_{CV}}{mkT} - 1 \right) \right], \quad (9)$$

[factors such as  $\dot{N}(E_L, E_H, T_C, 0)$  and  $\dot{N}(E_G, \infty, T_C, 0)$  are disregarded from previous equation, representing the negligible absorption from the thermal background], together with the following constrains:

$$eV = \mu_{CV} = \mu_{CI} + \mu_{IV} \quad (10)$$

$$\begin{aligned} &\xi\dot{N}(E_L, E_H, T_S, 0) - \dot{N}(E_L, E_H, T_C, \mu_{CI}) \\ &= \xi\dot{N}(E_H, E_G, T_S, 0) - \dot{N}(E_H, E_G, T_C, \mu_{IV}), \end{aligned} \quad (11)$$

which physically means that the net absorption across the  $E_L$  gap must equal that across the  $E_H$  gap. In these equations,  $T_S$  is the sun temperature (6000 K),  $e$  is the electron charge, and  $\xi$  is the photocurrent loss factor defined above. It will be easily realized that when  $\xi=1$  and  $J_0=0$ , the model set by Eqs. (9)–(11) correspond to the ideal IBSC model.<sup>1</sup> As part of the idealizations included in the model, these state also that the absorption coefficients ( $\alpha_{XY}$ ) that rule the photon absorption between bands (say from band  $X$  to band  $Y$ ) are selective. This means that, given a photon with energy  $\varepsilon$ , the probability of that photon being absorbed is dominant for the transition which is nearest in energy below  $\varepsilon$ .

However, to explore the impact of this idealization on the performance of the Cu(In,Ga)Se<sub>2</sub> cell being studied, we will now assume that the absorption coefficient for transitions from the IB to the CB overlap in the energy range  $E_L < \varepsilon < E_H$  with that of the transitions from the VB to the IB and that, in this range, both have the same magnitude ( $\alpha_{CI} = \alpha_{IV}$ ). As for the energy range  $\varepsilon > E_G$ , we still will assume that the absorption coefficient  $\alpha_{CV}$  is dominant. With this assumption, and considering that the thickness of the device tends to zero, it can be proven<sup>6,8</sup> that Eqs. (9)–(11) should be modified as follows:

$$J \approx e \left[ \dot{N}(E_L, E_H, T_S, 0) + \dot{N}(E_G, \infty, T_S, 0) + \frac{1}{2} \dot{N}(E_H, E_G, T_S, 0) \right] - e \left[ \dot{N}(E_L, E_H, T_C, \mu_{CI}) + \dot{N}(E_G, \infty, T_C, \mu_{CV}) \right. \\ \left. + \frac{1}{4} \dot{N}(E_H, E_G, T_C, \mu_{IC}) + \frac{1}{4} \dot{N}(E_H, E_G, T_C, \mu_{IV}) \right] - J_0 \left( \exp \frac{\mu_{CV}}{mkT} - 1 \right), \quad (12)$$

that has to be satisfied again together with Eq. (10) and now

$$\xi \dot{N}(E_L, E_H, T_S, 0) - \dot{N}(E_L, E_H, T_C, \mu_{CI}) = 0. \quad (13)$$

The resulting current-voltage characteristic has also been plotted in Fig. 5 where it has been labeled as “BB-IBSC (overlap).” Relevant performance parameters have been again included in the summary in Table II. The resulting efficiency is 19.2%, which leaves only 2.3 points for improvement when compared with the case in which the IB is not included (curve BB). This margin seems too low for a practical application of the IB to the improvement of a low-gap Cu(In,Ga)Se<sub>2</sub> cell, furthermore when considering that the interaction of the IB with other already existing defects would tend to reduce further the open-circuit voltage. On the other hand, the IB concept appears as a potential candidate to help improve the performance of wide-gap chalcopyrite solar cells, when observing the guidelines presented in the previous sections.

## V. CONCLUSIONS

We have explored the potential of the IB approach to increase the efficiency of thin-film-based solar cells. Due to the context in which this type of cells are usually operated, the analysis has considered that the operation of these cells takes place at one sun. From this perspective, it has been concluded that wide bandgap materials, such as CuGaS<sub>2</sub>, exhibit the highest room for improvement. In this case, the incorporation of donor Ti or acceptor Fe are pointed out as the transition metals with the highest potential to induce the formation of an intermediate band. In the radiative limit, no improvement is expected for materials with bandgaps below 1.14 eV by implementing an IB. However, when nonradiative recombination is present, this improvement is possible. This case has been discussed in detail for a Cu(In,Ga)Se<sub>2</sub> cell. The margin for improvement has been found small, about 6.4 points in idealized case, decreasing to only 2.3 points when the existence of other nonideal factors, such as the existence of overlapping between absorption coefficients, is considered.

## ACKNOWLEDGMENTS

This work has been supported by the European Commission within the project FULL-SPECTUM (SES6-CT-2003-502620) and the projects NUMANCIA (S-0505/ENE/000310) funded by the Comunidad de Madrid, and GENESIS FV (CSD2006-00004) funded by the Spanish National Programme. The authors acknowledge Professor J. C. Conesa and Professor P. Wahnón for valuable discussions. D.F.M. acknowledges financial support from the Spanish Ministry of Education and Science within the program Ramón y Cajal.

- <sup>1</sup>A. Luque and A. Martí, *Phys. Rev. Lett.* **78**, 5014 (1997).
- <sup>2</sup>J. S. Ward, K. Ramanathan, F. S. Hasoon, T. J. Coutts, J. Keane, M. A. Contreras, T. Moriarty, and R. Noufi, *Prog. Photovoltaics* **10**, 41 (2002).
- <sup>3</sup>S. B. Zhang, S. H. Wei, and A. Zunger, *Phys. Rev. Lett.* **78**, 4059 (1997).
- <sup>4</sup>C. Persson and A. Zunger, *Phys. Rev. Lett.* **91**, 266401 (2003).
- <sup>5</sup>A. Martí, E. Antolín, C. R. Stanley, C. D. Farmer, N. López, P. Diaz, E. Cánovas, P. G. Linares, and A. Luque, *Phys. Rev. Lett.* **97**, 247701 (2006).
- <sup>6</sup>A. Luque and A. Martí, *Prog. Photovoltaics* **9**, 73 (2001).
- <sup>7</sup>A. Luque, A. Martí, E. Antolín, and C. Tablero, *Physica B* **382**, 320 (2006).
- <sup>8</sup>L. Cuadra, A. Martí, and A. Luque, *IEEE Trans. Electron Devices* **51**, 1002 (2004).
- <sup>9</sup>M. Göppert-Mayer, *Ann. Phys.* **9**, 273 (1931).
- <sup>10</sup>T. F. Boggess, A. L. Smirl, S. C. Moss, I. W. Boyd, and E. W. van Stryland, *IEEE J. Quantum Electron.* **QE-21**, 488 (1985).
- <sup>11</sup>W. Denk, J. Strickler, and W. Webb, *Science* **248**, 73 (1990).
- <sup>12</sup>W. van Roosbroeck and W. Shockley, *Phys. Rev.* **94**, 1558 (1954).
- <sup>13</sup>W. Shockley and H. J. Queisser, *J. Appl. Phys.* **32**, 510 (1961).
- <sup>14</sup>G. L. Araújo and A. Martí, *Sol. Energy Mater. Sol. Cells* **33**, 213 (1994).
- <sup>15</sup>M. A. Contreras, K. Ramanathan, J. AbuShama, F. Hasson, D. L. Young, B. Egaas, and R. Noufi, *Prog. Photovoltaics* **13**, 209 (2005).
- <sup>16</sup>B. Tell, J. L. Shay, and H. M. Kasper, *J. Appl. Phys.* **43**, 2469 (1972).
- <sup>17</sup>J. L. Shay, B. Tell, and H. M. Kasper, *Appl. Phys. Lett.* **19**, 366 (1971).
- <sup>18</sup>A. Martí, L. Cuadra, and A. Luque, *Proceedings of the 28th IEEE Photovoltaics Specialists Conference* (IEEE, New York, 2000), pp. 189–234.
- <sup>19</sup>K. M. Yu, W. Walukiewicz, J. Wu, W. Shan, J. W. Beeman, M. A. Scarpulla, D. Dubon, and P. Becla, *Phys. Rev. Lett.* **91**, 246403 (2003).
- <sup>20</sup>K. M. Yu, W. Walukiewicz, J. W. Ager III, D. Bour, R. Farshchi, O. D. Dubon, S. X. Li, I. D. Sharp, and E. E. Haller, *Appl. Phys. Lett.* **88**, 092110 (2006).
- <sup>21</sup>M. Hamera, W. Walukiewicz, D. D. Nolte, and E. E. Haller, *Phys. Rev. B* **39**, 10114 (1989).
- <sup>22</sup>M. J. Caldas, A. Fazzio, and A. Zunger, *Appl. Phys. Lett.* **45**, 671 (1984).
- <sup>23</sup>K. A. Kikoin and V. N. Fleurov, *Transition Metal impurities in Semiconductors* (World Scientific, Singapore, 1994).
- <sup>24</sup>A. M. Hennel, *Transition Metals in III/V Compounds*, Semiconductors and Semimetals Vol. 38 (Academic, San Diego, 1993), Chap. 5, pp. 189–234.
- <sup>25</sup>M. Sugiyama and H. N. S. F. Chichibu, *Jpn. J. Appl. Phys., Part 2* **40**, L428 (2001).
- <sup>26</sup>S. M. Sze, *Physics of Semiconductor Devices*, 2nd ed. (Wiley, New York, 1981).
- <sup>27</sup>P. Palacios, K. Sanchez, J. C. Conesa, J. J. Fernandez, and P. Wahnón, *Thin Solid Films* **515**, 6280 (2007).
- <sup>28</sup>Y. J. Zhao and A. Zunger, *Phys. Rev. B* **69**, 104422 (2004).
- <sup>29</sup>C. Persson, Y. J. Zhao, S. Lany, and A. Zunger, *Phys. Rev. B* **72**, 035211 (2005).
- <sup>30</sup>J. M. Raulot, C. Domain, and J. F. Guillemoles, *Phys. Rev. B* **71**, 035203 (2005).
- <sup>31</sup>W. C. Zheng and S. Y. Wu, *J. Phys. Chem. Solids* **60**, 1725 (1999).
- <sup>32</sup>S. Shirakata, T. Terasako, E. Niwa, and K. Masumoto, *J. Phys. Chem. Solids* **64**, 1801 (2003).
- <sup>33</sup>K. Sakurai, H. Shibata, S. Nakamura, M. Yonemura, S. Kuwamori, Y. Kimura, S. Ishizuka, A. Yamada, K. Matsubara, H. Nakanishi, and S. Niki, in *Thin-film Compound Semiconductor Photovoltaics*, edited by W. Shafarman, T. Gessert, S. Niki, and S. Siebentritt (Mater. Res. Soc. Symp. Proc. 865, Warrendale, PA, 2005), F14.12.1.
- <sup>34</sup>S. Shirakata and S. Isomura, *Jpn. J. Appl. Phys., Part 1* **37**, 776 (1998).
- <sup>35</sup>I. Aksenov and K. Sato, *Jpn. J. Appl. Phys., Part 1* **31**, 2352 (1992).
- <sup>36</sup>T. Terasako, K. Hashimoto, Y. Nomoto, S. Shirakata, S. Isomura, E. Niwa, and K. Masumoto, *J. Lumin.* **87–89**, 1056 (2000).
- <sup>37</sup>W. N. Shafarman and L. Stolt, *Handbook of Photovoltaic Science and Engineering* (Wiley, New York, 2003), pp. 567–611.
- <sup>38</sup>R. Winston and W. T. Welford, *Optics of Non-Imaging Concentrators* (Academic, New York, 1979).